



UNIVERSITY OF LEEDS

This is a repository copy of *The relative contribution of orbital forcing and greenhouse gases to the North American deglaciation*.

White Rose Research Online URL for this paper:
<http://eprints.whiterose.ac.uk/92096/>

Version: Published Version

Article:

Gregoire, LJ, Valdes, PJ and Payne, AJ (2015) The relative contribution of orbital forcing and greenhouse gases to the North American deglaciation. *Geophysical Research Letters*, 42 (22). pp. 9970-9979. ISSN 0094-8276

<https://doi.org/10.1002/2015GL066005>

Reuse

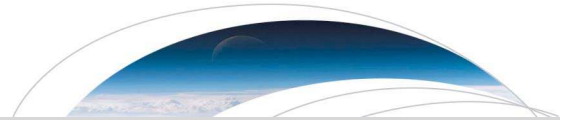
Unless indicated otherwise, fulltext items are protected by copyright with all rights reserved. The copyright exception in section 29 of the Copyright, Designs and Patents Act 1988 allows the making of a single copy solely for the purpose of non-commercial research or private study within the limits of fair dealing. The publisher or other rights-holder may allow further reproduction and re-use of this version - refer to the White Rose Research Online record for this item. Where records identify the publisher as the copyright holder, users can verify any specific terms of use on the publisher's website.

Takedown

If you consider content in White Rose Research Online to be in breach of UK law, please notify us by emailing eprints@whiterose.ac.uk including the URL of the record and the reason for the withdrawal request.



eprints@whiterose.ac.uk
<https://eprints.whiterose.ac.uk/>



RESEARCH LETTER

10.1002/2015GL066005

Key Points:

- We decompose the forcings of North American ice volume changes during the last deglaciation
- Orbital forcing drives 50%, greenhouse gases 30%, and forcing interactions 20% of the deglaciation
- The difference in timing of the forcings partly explains their relative contribution

Supporting Information:

- Supporting Information S1

Correspondence to:

L. J. Gregoire,
l.j.gregoire@leeds.ac.uk

Citation:

Gregoire, L. J., P. J. Valdes, and A. J. Payne (2015), The relative contribution of orbital forcing and greenhouse gases to the North American deglaciation, *Geophys. Res. Lett.*, *42*, doi:10.1002/2015GL066005.

Received 9 SEP 2015

Accepted 1 NOV 2015

Accepted article online 4 NOV 2015

The relative contribution of orbital forcing and greenhouse gases to the North American deglaciation

Lauren J. Gregoire¹, Paul J. Valdes², and Antony J. Payne²

¹School of Earth and Environment, University of Leeds, Leeds, UK, ²School of Geographical Sciences, University of Bristol, Bristol, UK

Abstract Understanding what drove Northern Hemisphere ice sheet melt during the last deglaciation (21–7 ka) can help constrain how sensitive contemporary ice sheets are to greenhouse gas (GHGs) changes. The roles of orbital forcing and GHGs in the deglaciation have previously been modeled but not yet quantified. Here for the first time we calculate the relative effect of these forcings on the North American deglaciation by driving a dynamical ice sheet model (GLIMMER-CISM) with a set of unaccelerated transient deglacial simulations with a full primitive equation-based ocean-atmosphere general circulation model (FAMOUS). We find that by 9 ka, orbital forcing has caused 50% of the deglaciation, GHG 30%, and the interaction between the two 20%. Orbital forcing starts affecting the ice volume at 19 ka, 2000 years before CO₂ starts increasing in our experiments, a delay which partly controls their relative effect.

1. Introduction

The last deglaciation (21–9 ka) was a period of major climate change, during which the demise of the North American and Eurasian ice sheets and retreat of the Greenland and Antarctic ice sheets resulted in the sea level rising by 130 m since 21 ka [Lambeck *et al.*, 2014]. According to the Milankovitch theory, the last deglaciation was caused by summer insolation increase at the latitude of the Northern Hemisphere ice sheets (45–80°N), starting around 23 ka [Milankovitch, 1941]. This was followed by an increase in atmospheric CO₂ concentrations, from 200 ppm at 19 ka to 260 ppm at 8 ka [Monnin *et al.*, 2001; Veres *et al.*, 2013], and an increase in CH₄ and N₂O concentrations [Spahni *et al.*, 2005], which further affected the climate. Quantifying the relative contribution of these forcings to the Northern Hemisphere ice sheet retreat can help us constrain the ice sheets sensitivity to increases in these gases.

The roles of orbital and atmospheric CO₂ changes in glacial-interglacial cycles have been investigated with a range of methods using simple theoretical models [e.g., Paillard, 1998], intermediate complexity models [e.g. Gallée *et al.*, 1992; Heinemann *et al.*, 2014], and parameterizations based on complex general circulation models [e.g. Abe-Ouchi *et al.*, 2013]. The difference in timescales and spatial scales of climate and ice sheet processes makes it difficult to model the full climate-ice sheet interaction with complex models, because of the length of model simulations required and because small climate model biases can produce large errors in ice volume [Pollard, 2000, 2010]. One way to overcome this is to use Earth system Models of Intermediate Complexity (EMICs) [Gallée *et al.*, 1992; Charbit *et al.*, 2005; Bonelli *et al.*, 2009; Ganopolski and Calov, 2011] in which atmospheric processes are simplified and resolved at very coarse resolution. Gallée *et al.* [1992] showed that deglaciation could be simulated with an EMIC, but required additional processes such as aging of snow albedo, while in Charbit *et al.* [2005], the Cordilleran sector did not fully deglaciate. Moreover, simplifications of the atmospheric component result in relatively crude simulations of precipitation and heavy use of downscaling techniques which introduce their own complexity.

More recently, using a slower, but more complex EMIC, LOVECLIM, coupled with a 3-D ice sheet model Heinemann *et al.* [2014] was able to simulate the last deglaciation. With a complex general circulation model (GCM), Abe-Ouchi *et al.* [2013] derived a sophisticated parameterization of glacial-interglacial climate evolution with ice sheet feedbacks. They showed that the geometry of the North American continent is key to explaining the timing of deglaciations.

These studies show that orbital changes are the primary driver of glacial-interglacial cycles [Ganopolski and Calov, 2011; Abe-Ouchi *et al.*, 2013]. Orbital changes also triggered [Heinemann *et al.*, 2014] and were the main driver of ice retreat [Charbit *et al.*, 2005] and climate change [He *et al.*, 2013] during the last deglaciation.

CO₂ has a secondary role in driving the glacial-interglacial cycles [Abe-Ouchi *et al.*, 2013] yet is crucial in controlling the amplitude of the cycles [Berger *et al.*, 1998; Ganopolski and Calov, 2011] and fully deglaciating North America [Charbit *et al.*, 2005; Heinemann *et al.*, 2014].

Despite this mechanistic understanding, the relative contributions of CO₂ and orbital forcings to deglacial ice retreat have not yet been quantified. Moreover, the timing and amplitude of CO₂ and orbital effects on ice sheets remains uncertain because of shortcomings in methodologies. For example, to compensate for their model's low climate sensitivity, Heinemann *et al.* [2014] artificially triple the radiative effect of CO₂. This bias correction makes the large assumption that the missing feedbacks that cause the low climate sensitivity (e.g., convective cloud feedback) only occur when climate change is forced by CO₂ and not by orbital changes. This potentially exaggerates the effect of CO₂. In the same study, the change in greenhouse gas concentrations and orbital parameters evolve 20 times faster than reality. This acceleration can affect the amplitude of changes and distort the leads and lags of the system [Lunt *et al.*, 2006] and may have slowed down the effect of CO₂ [Heinemann *et al.*, 2014]. Finally, the parameterization of glacial cycle climate from Abe-Ouchi *et al.* [2013] assumes a constant relationship through time and space between temperature and CO₂ and orbital forcings. This may introduce distortions in amplitude and timing of ice sheet changes.

We present the first quantification of the relative contribution of greenhouse gases (GHG) and orbital changes in the North American last deglaciation using transient simulations of the last deglaciation from a primitive equation-based coupled ocean-atmosphere GCM, FAMOUS, with no acceleration, bias correction, or additional parameterization of climate change. The climate simulations are forced with combinations of orbital, GHG, and geographical (sea level and ice sheet) changes and are used to drive the Glimmer-CISM ice sheet model offline. We use a factor decomposition technique to separate the contributions of these different forcings to the North American deglaciation. Since the ice sheet-climate feedbacks are prescribed as a forcing rather than being simulated, we quantify the uncertainty associated with transforming this ice forcing into a feedback.

2. Methodology

2.1. Ice Sheet Model

We model the North American ice sheet with the Glimmer-CISM 3-D thermomechanic ice sheet model version 1.0.14 [Rutt *et al.*, 2009]. The shallow ice approximation used in this version does not represent all marine ice sheet processes but allows for reasonably fast computation and is adequate for simulating the broad features of the North American ice sheet, where ocean-ice sheet interactions play a secondary role. The model performs well against EISMINT benchmarks [Rutt *et al.*, 2009] and has been used to simulate the Greenland ice sheet [Lunt *et al.*, 2008; Stone *et al.*, 2010] and the North American deglaciation [Gregoire *et al.*, 2012].

We use the same setup as Gregoire *et al.* [2012]. The North American ice sheet domain is represented by a 40 km Cartesian grid with 11 vertical sigma coordinate levels on a Lambeck azimuthal equal area projection [Snyder, 1987]. The mass balance is calculated with an annual positive degree day (PDD) scheme [Reeh, 1991] in which surface melting is proportional to the sum of positive degree day over a year. The PDD factors are set to 3 mm/d/°C for snow and 8 mm/d/°C for ice as in other studies [Marshall *et al.*, 2002; Charbit *et al.*, 2007; Bonelli *et al.*, 2009; Abe-Ouchi *et al.*, 2013; Heinemann *et al.*, 2014]. All precipitation is assumed to fall as snow, and up to 60% of meltwater can refreeze in the snow pack. To calculate the bedrock isostatic adjustment to the ice load, the solid Earth is represented as an elastic lithosphere floating on top of a relaxing mantle.

We start our experiments at the last glacial maximum (LGM; 21 ka), with ice thickness, extent, temperature, and velocity taken from spun-up LGM ice sheets as in Gregoire *et al.* [2012]. In this spin-up, we interpolated between the FAMOUS present day and LGM equilibrium climate with a climate index based on a Greenland ice core record $\delta^{18}\text{O}$ record [NGRIP Members, 2004] and use the interpolated climate to built-up the ice sheet through the last glacial cycle (120–21 ka). Ice is allowed to advance on shallow basins and calving occurs only where the bathymetry is deeper than 500 m. In the subsequent deglacial experiment, calving occurs when ice reaches a floating point. The main tuneable model parameters (basal sliding, flow factor, lapse rate, PDD factors, and mantle relaxation time) were previously adjusted to optimize ice volume and area at the LGM compared to the ice-5G reconstruction [Gregoire, 2010] (see Table S1 in the supporting information). The resulting LGM North American ice sheet has a volume of $3.5 \times 10^6 \text{ km}^3$ (7% larger than ICE-5G) over $16 \times 10^6 \text{ km}^2$ (4% less than Ice-5G).

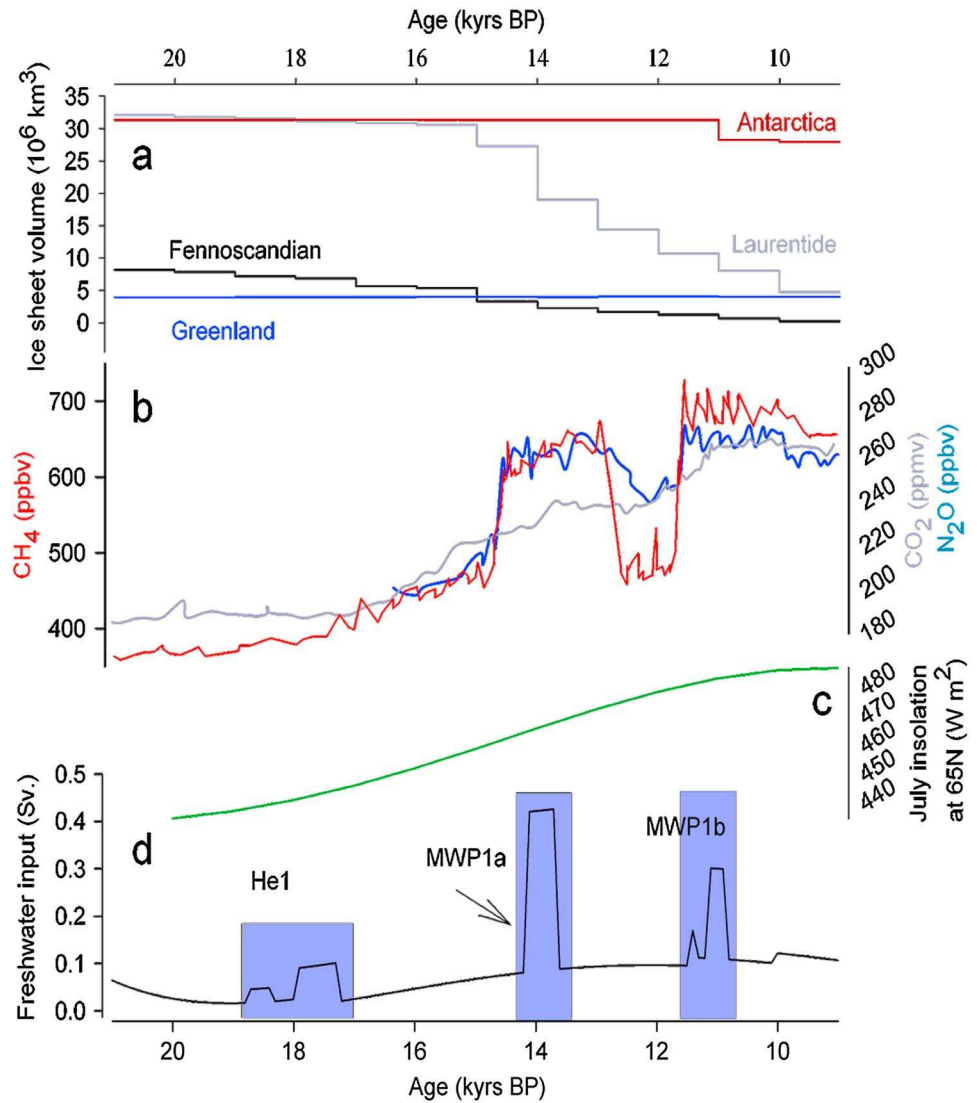


Figure 1. Boundary condition for the FAMOUS deglacial climate simulation. (a) Ice-5G ice sheet volume [Peltier, 2004], (b) atmospheric trace gases concentration [Monnin et al., 2001; Spahni et al., 2005], (c) July insolation at 65°N [Berger and Loutre, 1992], and (d) freshwater flux.

2.2. Climate Forcing

To force the ice sheet model through the deglaciation, we use monthly mean temperature and precipitation from a set of transient simulations of the last deglaciation as in Gregoire et al. [2012]. In these runs, ice sheet extent, bathymetry, orography, and the land-sea mask are updated every 1000 years based on Ice-5G [Peltier, 2004]. The vegetation is held constant at the present-day values, except for area covered by ice. Similarly, aerosols are held constant throughout the run. CO_2 , CH_4 , and N_2O concentrations are varied every time step with values taken from European Project for Ice Coring in Antarctica Dome C on the original chronologies [Monnin et al., 2001; Spahni et al., 2005] (Figure 1). The simulations are forced with continuously varying insolation at the top of the atmosphere taken from Berger and Loutre [1992]. The freshwater flux to the oceans, produced as part of the ORMEN project, consists of a background flux from ice sheet melt and three meltwater pulses (Figure 1).

We use five experiments with different combinations of climate forcing: (1) GEOG: changes in geography are prescribed, and other boundary conditions are fixed to those of the LGM; (2) GEOG_ORB: the geography and orbital parameters are changed; (3) GEOG_GHG: the geography and trace gases concentrations are changed; (4) GEOG_ORB_GHG: the geography, orbital parameters, and trace gases concentrations are changed; and (5) ALL: includes all the above changes and the additional freshwater forcing.

With all the forcings included (ALL), global temperatures warm by 4.2°C between 21 ka and 9 ka. The model simulates the appropriate LGM temperature and subsequent warming over Greenland compared to the Greenland Ice Sheet Project Two record [Alley, 2004] but shows a much smaller variability in the climate change (Figure S1). In particular, the model does not simulate the rapid Bølling warming and the Younger-Dryas cold event [Alley, 2004]. Possible explanations for this are (i) that the freshwater forcing used here is missing some key fluxes or that these are put in the wrong locations, (ii) that the ocean circulation in FAMOUS is not sensitive enough to the forcings, or (iii) simply that the climate changes are caused by another factor not included in our model. The lack of large rapid change in our climate forcing could impact the resulting temporal evolution of ice volume. However, the model produces the correct range of temperature change in Greenland, which suggests it simulates well the overall deglacial climate change.

We use monthly precipitation and temperatures from these transient simulations to force the ice sheet model. Orography is also input into the ice sheet model to downscale the temperature field onto the ice sheet grids using a 5°C/km constant lapse rate. We do not make any corrections to the precipitation as the field is already consistent with the climate model orography taken from Ice-5G.

In our control experiment (CTRL) we keep the climate fixed at the LGM for 12,000 years. Other ice sheet experiments are referred to by the name of their forcing climate simulation: GEOG, GEOG_ORB, GEOG_GHG, GEOG_ORB_GHG, and ALL. We have six experiments including the control CTRL.

2.3. Factor Decomposition

Using CTRL, GEOG, GEOG_ORB, GEOG_GHG, and GEOG_ORB_GHG, we decompose the effects of changes in geography (GEOG), orbital parameters (ORB), and GHG on the total North American ice volume [Stein and Alpert, 1993]. We, respectively, call V_i , V_{ij} , and V_{ijk} the North American ice volume when the factor(s) i , i and j , or i , j , and k are considered. We call \widehat{V}_i the fraction of V induced by the factor i . The factor \widehat{V}_{ijk} is therefore the contribution of the pure triple interaction between i , j , and k . We name the geography forcings I (for ice), the orbital forcing O , and the greenhouse gases forcing G . Following this notation, the North American ice volume in the simulations CTRL, GEOG, GEOG_ORB, GEOG_GHG, and GEOG_ORB_GHG is written V_C , V_I , V_{IO} , V_{IG} , and V_{IOG} , respectively. Ice volume change in each experiment can be decomposed in the following way:

$$\begin{aligned}
 V_C &= \widehat{V}_C \\
 V_I &= \widehat{V}_I + \widehat{V}_C \\
 V_{IO} &= \widehat{V}_I + \widehat{V}_O + \widehat{V}_{IO} + \widehat{V}_C \\
 V_{IG} &= \widehat{V}_I + \widehat{V}_G + \widehat{V}_{IG} + \widehat{V}_C \\
 V_{IOG} &= \widehat{V}_I + \widehat{V}_O + \widehat{V}_G + \widehat{V}_{IO} + \widehat{V}_{IG} + \widehat{V}_{OG} + \widehat{V}_{IOG} + \widehat{V}_C
 \end{aligned} \tag{1}$$

With five simulations (including the control), we do not fully solve our system of equations [Stein and Alpert, 1993], but we can separate the effect of the three factors by rearranging the previous equations. For convenience, we represent the ice volume lost since the LGM by multiplying the equations by -1 . We therefore express the contributions of geography (ICE), orbital forcing (ORB), and GHG to the ice volume lost through time, as follows:

$$\begin{aligned}
 \text{ICE}(t) &= -\widehat{V}_I(t) = V_C(t) - V_I(t) \\
 \text{ORB}(t) &= -(\widehat{V}_O(t) + \widehat{V}_{IO}(t)) = V_I(t) - V_{IO}(t) \\
 \text{GHG}(t) &= -(\widehat{V}_G(t) + \widehat{V}_{IG}(t)) = V_I(t) - V_{IG}(t)
 \end{aligned} \tag{2}$$

Here ORB and GHG include the effect of interactions between geography and orbit, and geography and GHG. We also define the total ice volume loss through time as

$$\text{TOTAL}(t) = V_C(t) - V_{IOG}(t), \tag{3}$$

which can be expressed as the sum of ICE, ORB, and GHG, plus a term involving interactions between orbital and GHG forcings:

$$\text{TOTAL}(t) = \text{ICE}(t) + \text{ORB}(t) + \text{GHG}(t) + \text{Int}(t), \tag{4}$$

with

$$\text{Int}(t) = \widehat{V}_{OG}(t) + \widehat{V}_{IOG}(t). \tag{5}$$

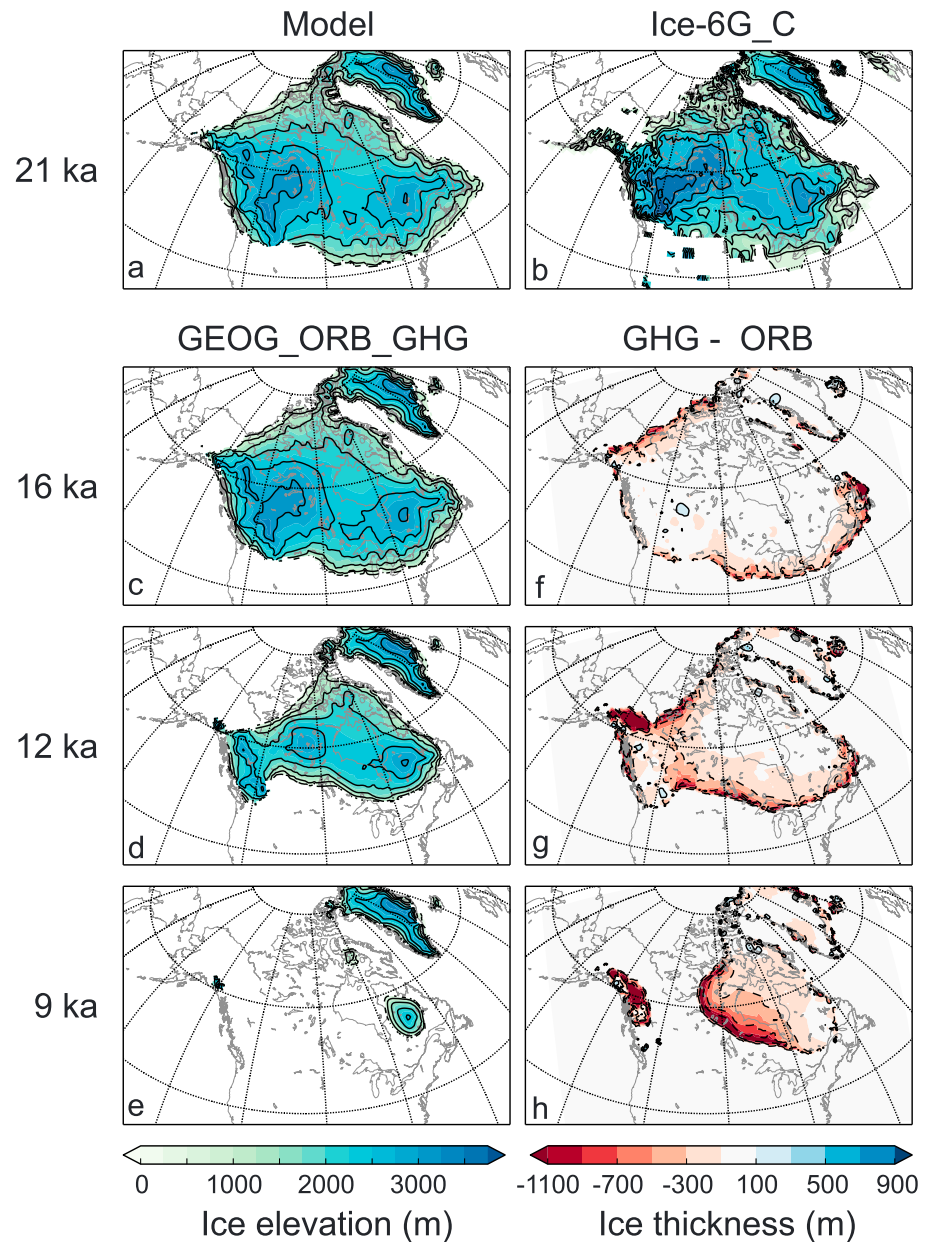


Figure 2. Ice surface elevation of (a) the model initial condition (21 ka), (b) Ice-6G_C at 21 ka [Peltier et al., 2015], and (c–e) GEOG_ORB_GHG experiment at 16, 12, and 9 ka. Difference in ice thickness in meters (f and g) between the GEOG_GHG experiment and the GEOG_ORB experiment (GEOG_GHG–GEOG_ORB) at 16, 12, and 9 ka. Red colours indicate areas where orbital forcing has caused a greater ice loss than GHG changes.

3. Results and Discussion

3.1. Evaluation

With all forcings included, the extent of the North American ice sheet modeled through the deglaciation matches well the reconstruction of Dyke [2004], also used in the Ice-5G reconstruction [Peltier, 2004]. This is partly because Ice-5G is used as an input to our climate experiments. Ice thickness and surface elevation on the other hand differ from Ice-5G but are similar to the newer Ice-6G_C reconstruction [Peltier et al., 2015] (Figures 2a and 2b) and the reconstruction of Tarasov and Peltier [2006] (not shown).

The Cordilleran and Laurentide ice sheets separate late, around 11.6 ka instead of ~14.5 ka in Dyke [2004]. This delay is as yet unexplained [Gregoire et al., 2012], but interestingly, other modeling studies report a similar

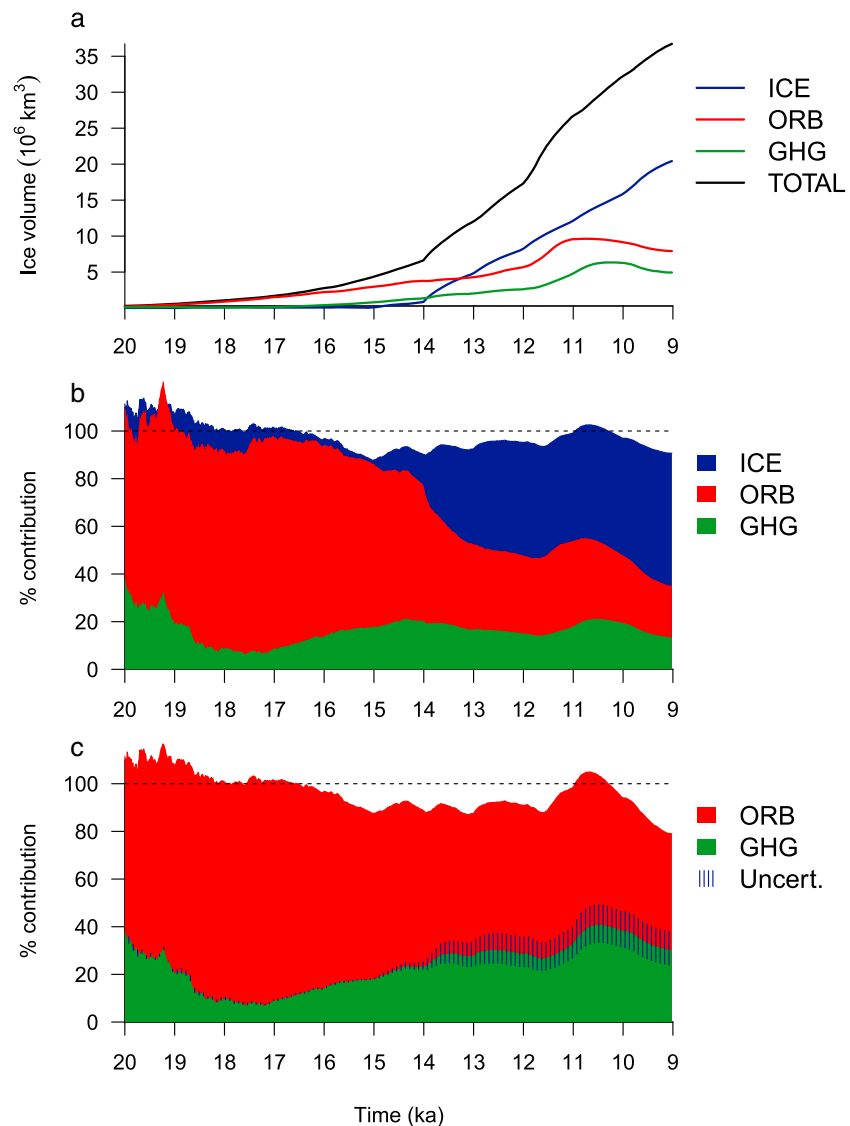


Figure 3. Contributions to North American ice volume lost through the deglaciation due to each forcing expressed (a) as ice volumes calculated from equations (2) and (3), (b) as a percentage of the total volume loss (TOTAL in equation (3)), and (c) as a percentage contribution when ICE is considered as a feedback. The blue vertical lines represent the uncertainty associated with representing ICE as a feedback (Text S2).

timing for this separation [Abe-Ouchi *et al.*, 2013; Heinemann *et al.*, 2014]. Despite the delay, the continent is completely deglaciated by 6 ka as in Dyke [2004]. We therefore simulate well the duration and rate of the deglaciation on North America, giving us confidence that processes involved in the overall deglaciation are well represented (more details in Gregoire *et al.* [2012]).

3.2. Effect of Geography

Part of the ice retreat in the model is driven by the geographical changes prescribed in the climate experiments (ICE in Figure 3), involving bathymetry, orography, coastlines, and ice sheet extent and elevation. Additional climate model simulations (W. H. G. Roberts, personal communication) suggest that the dominant components of these “geography” changes are the ice sheet extent and elevation. The bathymetry and coastline changes generally have a much smaller impact on climate. The changes in ICE-5G extent and elevation modify the albedo and atmospheric (and potentially oceanic) circulation resulting in changes to temperature and precipitation and hence changes in ice sheet surface mass balance. The ICE contribution only becomes large after 14 ka because ice sheet extent only starts significantly changing at this time (Figure 1).

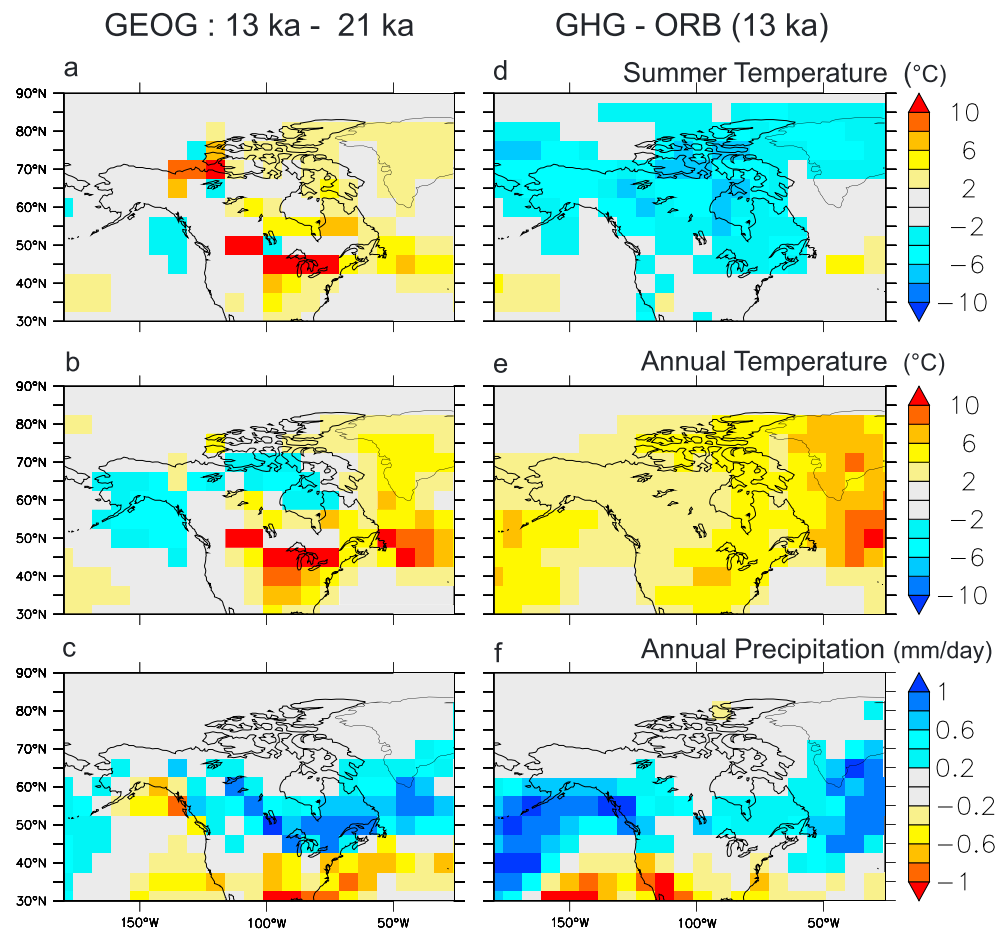


Figure 4. (a–c) Impact of geography and (d–f) comparison of orbital, greenhouse gases effect on June to August mean temperature in °C (Figures 4a and 4d), annual mean temperature in °C (Figures 4b and 4e), and annual mean precipitation in mm/d (Figures 4c and 4f). Figures 4a–4c show the GEOG experiment at 13 ka minus 21 ka. Figures 4d–4f show climatologies of GEOG_GHG minus GEOG_ORB at 13 ka. Temperatures are corrected for changes in elevation using a lapse rate of 5°C/km.

Over the deglaciation, geographical changes produce an average 3°C summer warming over North America between 21 and 13 ka (Figure 4a). Where the ice margin has retreated, the warming can exceed 10°C and precipitation increases (Figures 4a and 4c). Because ice extent is updated every 1000 years in our climate experiments, ice sheet melt increases sharply at these intervals, especially at 14, 13, 12, and 10 ka.

By 9 ka, the ICE forcing accounts for around half the North American ice loss (Figure 3b). This shows that this feedback process significantly amplifies the GHG and orbital changes. In a coupled ice-climate system these geographical changes would have been caused by orbital or GHG forcings alone. The ICE component can therefore be seen as representing ice-climate feedbacks, and we can recalculate the relative contributions of ORB and GHG with ICE as a feedback (Figure 3c and Text S2). These feedbacks mostly involve ice albedo and atmospheric circulation, since ice elevation is corrected for with a fixed lapse rate.

3.3. Effects of CO₂ and Orbital Forcings

Even though greenhouse gas changes produce a greater annual mean warming than the orbital forcing between 21 ka and 13 ka (Figure 4e), they produce a much weaker summer warming (Figure 4d). Hence, we would expect orbital forcing to have a larger impact on the North American ice sheet, since ice sheet mass balance is mostly controlled by the summer melting season [Milankovitch, 1941].

Orbital changes start noticeably affecting the North American ice volume at 19 ka, while the effect of GHG only starts to be significant at 16 ka (Figure 3a). After 16 ka, the sum of ORB and GHG is mostly lower than 100% of

TOTAL (Figure 3c); this means that the remaining interactive term $\text{Int}(t)$ is positive. This is due to the nonlinearity of the ice sheet response to climate forcings, which in this instance likely originate from a surface mass balance-elevation feedback acting to reinforce the deglaciation. The relative contribution of orbital forcing peaks at 10.9 ka and that of GHG peaks at 9.6 ka, when the Cordilleran and Laurentide ice sheet separate, which causes an acceleration of the ice melt (Figure S2) due to the saddle collapse mechanism [Gregoire *et al.*, 2012]. The difference in the timing of the separation is what temporarily increases the relative contribution of the forcings and causes the interactive term $\text{Int}(t)$ to be negative around 10.5 ka (Figures 3b and 3c).

By 9 ka, the orbital forcing has contributed 50% and the greenhouse gas forcing 30% to the North American deglaciation, if we consider the geographical changes (ICE) as a feedback in the climate system (Figure 3c). The remaining 20% of the deglaciation is caused by interactions between the forcings. These results are for the case where the ICE feedback is assumed to be the same for all forcings (Text S2). However, this may not be the case because orbital and GHG forcings affect the climate differently both seasonally and spatially (Figures 4d–4f). Based on extreme cases where the ICE feedback is twice and half as strong for one forcing than the other (Text S2), we find that the contributions of orbital and GHG forcings vary by $\pm 7\%$ (blue bars in Figure 3c).

The relative contributions of orbital and GHG forcings to ice volume changes vary over time (Figure 3c). From 16 to 9 ka, the average mass balance is the same in GEOG_ORB and GEOG_GHG (Figure S2) meaning that the effects of orbital and greenhouse gas forcings are equivalent over that period. Orbital and GHG forcings also produce similar patterns of ice retreat; the differences in ice thickness between the GEOG_ORB and GEOG_GHG experiments follow the pattern of deglacial ice retreat (Figures 2c–2g). Therefore, these differences mostly reflect a delay in the GEOG_GHG deglaciation compared to GEOG_ORB. This suggests that orbital forcing contributes more to the deglaciation partly because orbital forcing starts changing before CO_2 .

The recent Antarctic ice core chronology 2012 ice core chronologies [Parrenin *et al.*, 2013] date the initial CO_2 increase 1600 years earlier than in the Monnin *et al.* [2001] record used in our climate simulations. Therefore, the effect of CO_2 on ice retreat may be delayed and underestimated in our results. This late CO_2 increase could partly explain why the Laurentide and Cordilleran ice sheets separate 2500 years late in our model and other studies. This delay could also be caused by missing or misrepresented processes in our model. For example, the shallow ice approximation used here does not fully represent ice stream dynamic. More complex and slower ice sheet models are required to correctly simulate this. Also, the positive degree day mass balance scheme does not explicitly account for the effect of shortwave radiation changes on the ice sheet mass balance [Robinson *et al.*, 2010; van de Berg *et al.*, 2011] which could lead to the orbital forcing being underestimated here.

3.4. The Additional Effect of Meltwater

Ice sheet and iceberg meltwater entering the oceans generally has little impact on the climate simulated by FAMOUS, except for a weakening in the Atlantic Overturning Circulation from 20 sverdrup (Sv) to 12 Sv around 14.5 ka due to the meltwater pulse 1a freshwater pulse, resulting in a $\sim 1^\circ\text{C}$ cooling in northeast Canada and the Hudson Bay region (not shown). This delays the North American deglaciation by 700 years. As mentioned earlier, the ALL FAMOUS experiment does not reproduce the details of the rapid cooling and warming patterns of the deglaciation [Alley, 2004]; it is therefore possible that the effect of freshwater on the climate is not well represented in our model.

4. Conclusions

We have calculated the relative effect of CO_2 and orbital forcings on the North American deglaciation by forcing a dynamic ice sheet model with a set of fully transient deglacial simulations from a GCM and performing a factor decomposition on the results.

We find that orbital forcing explains $50\% \pm 7\%$ of the reduction in North American ice volume, while GHG increases, which include CO_2 , explain $30\% \pm 7\%$ of this deglaciation. We suggest that the relative contribution of these forcings is partly controlled by the relative timing of the forcings. In our experiments, orbital forcing starts affecting the ice volume at 19 ka, 3000 years before the CO_2 forcing does. The reduction in ice sheet elevation and extent adds a further major feedback on to the climate change.

Our results agree well with other studies [Ganopolski and Calov, 2011; Abe-Ouchi et al., 2013; He et al., 2013; Heinemann et al., 2014] in terms of the timing of initiation and of the role of orbital forcing and CO₂. In addition, we are able to go a step further and quantify the relative contributions of these forcings. Further work using fully coupled runs of the last deglaciation with a similar general circulation model and an energy mass balance scheme would be needed to confirm the results.

Acknowledgments

This work was supported by the Marie Curie Research Training Network NICE (MRTN-CT-2006-036127) and the NERC projects NE/D001846/1, NE/C509558/1, and NE/G006989/1. Glimmer-CISM was developed within the NERC National Centre for Earth Observation. The numerical simulations were carried out using the computational facilities of the BRIDGE and Leeds palaeo@Leeds groups and those of the Advanced Computing Research Centre, University of Bristol (<http://www.bris.ac.uk/acrc/>). The model output data presented here are available on request.

References

- Abe-Ouchi, A., F. Saito, K. Kawamura, M. E. Raymo, J. Okuno, K. Takahashi, and H. Blatter (2013), Insolation-driven 100,000-year glacial cycles and hysteresis of ice-sheet volume, *Nature*, *500*(7461), 190–193, doi:10.1038/nature12374.
- Alley, R. B. (2004), *GISP2 Ice Core Temperature and Accumulation Data*, *Data Contrib. Ser.*, IGBP PAGES/World Data Cent. for Paleoclimatol., Boulder, Colo.
- Berger, A., and M. F. Loutre (1992), Astronomical solutions for paleoclimate studies over the last 3 million years, *Earth Planet. Sci. Lett.*, *111*(2–4), 369–382, doi:10.1016/0012-821X(92)90190-7.
- Berger, A., H. Gallee, and X. S. Li (1998), Ice-sheet growth and high-latitudes sea-surface temperature, *Oceanogr. Lit. Rev.*, *1*(45), 36.
- Bonelli, S., S. Charbit, M. Kageyama, M.-N. Woillez, G. Ramstein, C. Dumas, and A. Quiquet (2009), Investigating the evolution of major Northern Hemisphere ice sheets during the last glacial-interglacial cycle, *Clim. Past*, *5*(3), 329–345, doi:10.5194/cp-5-329-2009.
- Charbit, S., M. Kageyama, D. Roche, C. Ritz, and G. Ramstein (2005), Investigating the mechanisms leading to the deglaciation of past continental northern hemisphere ice sheets with the CLIMBER-GREMLINS coupled model, *Global Planet. Change*, *48*(4), 253–273.
- Charbit, S., C. Ritz, G. Philippon, V. Peyaud, and M. Kageyama (2007), Numerical reconstructions of the Northern Hemisphere ice sheets through the last glacial-interglacial cycle, *Clim. Past*, *3*(1), 15–37, doi:10.5194/cp-3-15-2007.
- Dyke, A. S. (2004), An outline of North American deglaciation with emphasis on central and northern Canada, in *Quaternary Glaciations—Extent and Chronology—Part II: North America, Part 2*, vol. 2, pp. 373–424, Elsevier, Amsterdam.
- Gallée, H., J. P. Van Ypersele, T. Fichefet, I. Marsiat, C. Tricot, and A. Berger (1992), Simulation of the last glacial cycle by a coupled, sectorially averaged climate-ice sheet model: 2. Response to insolation and CO₂ variations, *J. Geophys. Res.*, *97*, 15,713–15,740, doi:10.1029/92JD01256.
- Ganopolski, A., and R. Calov (2011), The role of orbital forcing, carbon dioxide and regolith in 100 kyr glacial cycles, *Clim. Past*, *7*(4), 1415–1425, doi:10.5194/cp-7-1415-2011.
- Gregoire, L. J. (2010), Modelling the Northern Hemisphere climate and Ice sheets during the last deglaciation, PhD thesis, Univ. of Bristol, Bristol, U. K., Dec.
- Gregoire, L. J., A. J. Payne, and P. J. Valdes (2012), Deglacial rapid sea level rises caused by ice-sheet saddle collapses, *Nature*, *487*(7406), 219–222, doi:10.1038/nature11257.
- He, F., J. D. Shakun, P. U. Clark, A. E. Carlson, Z. Liu, B. L. Otto-Bliesner, and J. E. Kutzbach (2013), Northern Hemisphere forcing of Southern Hemisphere climate during the last deglaciation, *Nature*, *494*(7435), 81–85, doi:10.1038/nature11822.
- Heinemann, M., A. Timmermann, O. Elison Timm, F. Saito, and A. Abe-Ouchi (2014), Deglacial ice sheet meltdown: Orbital pacemaking and CO₂ effects, *Clim. Past*, *10*(4), 1567–1579, doi:10.5194/cp-10-1567-2014.
- Lambeck, K., H. Rouby, A. Purcell, Y. Sun, and M. Sambridge (2014), Sea level and global ice volumes from the Last Glacial Maximum to the Holocene, *Proc. Natl. Acad. Sci. U.S.A.*, *111*(43), 15,296–15,303, doi:10.1073/pnas.1411762111.
- Lunt, D. J., M. S. Williamson, P. Valdes, and T. M. Lenton (2006), Comparing transient, accelerated, and equilibrium simulations of the last 30,000 years with the GENIE-1 model, *Clim. Past*, *2*, 221–235.
- Lunt, D. J., G. L. Foster, A. M. Haywood, and E. J. Stone (2008), Late Pliocene Greenland glaciation controlled by a decline in atmospheric CO₂ levels, *Nature*, *454*(7208), 1102–1105, doi:10.1038/nature07223.
- Marshall, S. J., T. S. James, and G. K. C. Clarke (2002), North American ice sheet reconstructions at the Last Glacial Maximum, *Quat. Sci. Rev.*, *21*(1–3), 175–192, doi:10.1016/S0277-3791(01)00089-0.
- Milankovitch, M. (1941), *Kanon der Erdbeustrahlungen und seine Anwendung auf das Eiszeitenproblem [English Translation: Canon of Insolation and the Ice Age Problem]*, Alven Global, Belgrade.
- Monnin, E., A. Indermuhle, A. Dallenbach, J. Fluckiger, B. Stauffer, T. F. Stocker, D. Raynaud, and J. M. Barnola (2001), Atmospheric CO₂ concentrations over the last glacial termination, *Science*, *291*(5501), 112–114.
- NGRIP Members (2004), High-resolution record of Northern Hemisphere climate extending into the last interglacial period, *Nature*, *431*(7005), 147–151, doi:10.1038/nature02805.
- Paillard, D. (1998), The timing of Pleistocene glaciations from a simple multiple-state climate model, *Nature*, *391*(6665), 378–381, doi:10.1038/34891.
- Parrenin, F., V. Masson-Delmotte, P. Köhler, D. Raynaud, D. Paillard, J. Schwander, C. Barbante, A. Landais, A. Wegner, and J. Jouzel (2013), Synchronous change of atmospheric CO₂ and Antarctic temperature during the last deglacial warming, *Science*, *339*(6123), 1060–1063, doi:10.1126/science.1226368.
- Peltier, W. R. (2004), Global glacial isostasy and the surface of the ice-age earth: The ice-5G (VM2) model and grace, *Annu. Rev. Earth Planet. Sci.*, *32*, 111–149.
- Peltier, W. R., D. F. Argus, and R. Drummond (2015), Space geodesy constrains ice age terminal deglaciation: The global ICE-6G_C (VM5a) model, *J. Geophys. Res. Solid Earth*, *120*, 450–487, doi:10.1002/2014JB011176.
- Pollard, D. (2000), Comparisons of ice-sheet surface mass budgets from Paleoclimate Modeling Intercomparison Project (PMIP) simulations, *Global Planet. Change*, *24*(2), 79–106, doi:10.1016/S0921-8181(99)00071-5.
- Pollard, D. (2010), A retrospective look at coupled ice sheet–climate modeling, *Clim. Change*, *100*(1), 173–194, doi:10.1007/s10584-010-9830-9.
- Reeh, N. (1991), Parameterization of melt rate and surface temperature in the Greenland ice sheet, *Polarforschung*, *59*(3), 113–128.
- Robinson, A., R. Calov, and A. Ganopolski (2010), An efficient regional energy–moisture balance model for simulation of the Greenland ice sheet response to climate change, *Cryosphere*, *4*(2), 129–144, doi:10.5194/tc-4-129-2010.
- Rutt, I. C., M. Haggdorn, N. R. J. Hulton, and A. J. Payne (2009), The Glimmer community ice sheet model, *J. Geophys. Res.*, *114*, F02004, doi:10.1029/2008JF001015.
- Snyder, J. P. (1987), *Map Projections: A Working Manual*, U.S. Geol. Surv. Prof. Pap., 1395, U.S. Gov. Print. Off., Washington, D. C.
- Spahni, R., et al. (2005), Atmospheric methane and nitrous oxide of the Late Pleistocene from Antarctic ice cores, *Science*, *310*(5752), 1317–1321, doi:10.1126/science.1120132.

- Stein, U., and P. Alpert (1993), Factor separation in numerical simulations, *J. Atmos. Sci.*, *50*(14), 2107–2115.
- Stone, E. J., D. J. Lunt, I. C. Rutt, and E. Hanna (2010), Investigating the sensitivity of numerical model simulations of the modern state of the Greenland ice-sheet and its future response to climate change, *Cryosphere*, *4*(3), 397–417, doi:10.5194/tc-4-397-2010.
- Tarasov, L., and W. R. Peltier (2006), A calibrated deglacial drainage chronology for the North American continent: Evidence of an Arctic trigger for the Younger Dryas, *Quat. Sci. Rev.*, *25*(7–8), 659–688, doi:10.1016/j.quascirev.2005.12.006.
- Van de Berg, W. J., M. van den Broeke, J. Ettema, E. van Meijgaard, and F. Kaspar (2011), Significant contribution of insolation to Eemian melting of the Greenland ice sheet, *Nat. Geosci.*, *4*(10), 679–683, doi:10.1038/ngeo1245.
- Veres, D., et al. (2013), The Antarctic ice core chronology (AICC2012): An optimized multi-parameter and multi-site dating approach for the last 120 thousand years, *Clim. Past*, *9*(4), 1733–1748, doi:10.5194/cp-9-1733-2013.